

Cavity enhanced nonlinear optics for few photon optical bistability

Taylor K. Fryett, Christopher M. Dodson, and Arka Majumdar*

Department of Electrical Engineering, University of Washington, Seattle, WA 98195 USA

*arka@uw.edu

Abstract: Weak material nonlinearity at optical frequencies poses a serious hurdle to realizing optical bistability at low optical powers, which is a critical component for digital optical computing. In this paper, we explore the cavity enhancement of the second-order optical nonlinearity in order to determine the feasibility of few photon optical bistability. Starting from a quantum optical formalism of a doubly resonant cavity (required to meet the condition of phase matching), we derive a dynamic classical model of a cavity that is bistable at the fundamental mode. We analyze the optical energy and the switching speed as a function of the cavity quality factors and mode volumes and identify the regime where only ten's of photons are required to perform the switching. An unusual trend in the switching speed is also observed, where the speed monotonically decreases as the cavity linewidth increases. This is ascribed to the increase in the switching gain with increasing cavity linewidth.

© 2015 Optical Society of America

OCIS codes: (190.1450) Bistability; (130.0130) Integrated optics; (130.3750) Optical logic devices; (200.0200) Optics in computing; (190.0190) Nonlinear optics.

References and links

1. A. Sawchuk and T. C. Strand, "Digital optical computing," *Proceedings of the IEEE* **72**, 758–779 (1984).
2. H. Gibbs, *Optical Bistability: Controlling Light with Light* (Academic Press, 1985).
3. D. A. B. Miller, "Are optical transistors the logical next step?" *Nature Photonics* **4**, 3–5 (2010).
4. H. J. Caulfield and S. Dolev, "Why future supercomputing requires optics," *Nature Photonics* **4**, 261–263 (2014).
5. V. R. Almeida and M. Lipson, "Optical bistability on a silicon chip," *Opt. Lett.* **29**, 2387–2389 (2004).
6. K. Nozaki, A. Shinya, S. Matsuo, Y. Suzuki, T. Segawa, T. Sato, Y. Kawaguchi, R. Takahashi, and M. Notomi, "Ultralow-power all-optical ram based on nanocavities," *Nature Photonics* **6**, 248252 (2012).
7. M. Sodagar, M. Miri, A. A. Eftekhar, and A. Adibi, "Optical bistability in a one-dimensional photonic crystal resonator using a reverse-biased pn-junction," *Opt. Express* **23**, 2676–2685 (2015).
8. A. Majumdar and A. Rundquist, "Cavity-enabled self-electro-optic bistability in silicon photonics," *Opt. Lett.* **39**, 3864–3867 (2014).
9. Y.-D. Kwon, M. A. Armen, and H. Mabuchi, "Femtojoule-scale all-optical latching and modulation via cavity nonlinear optics," *Phys. Rev. Lett.* **111**, 203002 (2013).
10. M. Soljačić, E. Lidorikis, M. Ibanescu, S. G. Johnson, J. Joannopoulos, and Y. Fink, "Optical bistability and cutoff solitons in photonic bandgap fibers," *Opt. Express* **12**, 1518–1527 (2004).
11. M. Hochberg and T. Baehr-Jones, "Towards fabless silicon photonics," *Nature Photonics* **4**, 492–494 (2010).
12. D. J. Moss, R. Morandotti, A. L. Gaeta, and M. Lipson, "New cmos-compatible platforms based on silicon nitride and hydrex for nonlinear optics," *Nature Photonics* **7**, 597607 (2013).
13. L. M. Malard, T. V. Alencar, A. P. M. Barboza, K. F. Mak, and A. M. de Paula, "Observation of intense second harmonic generation from mos₂ atomic crystals," *Phys. Rev. B* **87**, 201401 (2013).
14. J. Wang, H. Mabuchi, and X.-L. Qi, "Calculation of divergent photon absorption in ultrathin films of a topological insulator," *Phys. Rev. B* **88**, 195127 (2013).
15. R. Boyd, *Nonlinear optics* (Academic Press, 2008).
16. K. Rivoire, Z. Lin, F. Hatami, W. T. Masselink, and J. Vučković, "Second harmonic generation in gallium phosphide photonic crystal nanocavities with ultralow continuous wave pump power," *Opt. Express* **17**, 22609–22615 (2009).

17. S. Buckley, M. Radulaski, J. L. Zhang, J. Petykiewicz, K. Biermann, and J. Vučković, "Multimode nanobeam cavities for nonlinear optics: high quality resonances separated by an octave," *Opt. Express* **22**, 26498–26509 (2014).
 18. A. Majumdar and D. Gerace, "Single-photon blockade in doubly resonant nanocavities with second-order nonlinearity," *Physical Review B* **87** 235319 (2013).
 19. A. Majumdar, M. Bajcsy, D. Englund, and J. Vuckovic, "All optical switching with a single quantum dot strongly coupled to a photonic crystal cavity," *Selected Topics in Quantum Electronics, IEEE Journal of* **18**, 1812–1817 (2012).
 20. C. W. Gardiner and P. Zoller, *Quantum Noise* (Springer-Verlag, 2005).
 21. C. Janisch, Y. Wang, D. Ma, N. Mehta, A. L. Elias, N. Perea-Lopez, M. Terrones, V. Crespi, and Z. Liu, "Extraordinary second harmonic generation in tungsten disulfide monolayers," *Scientific Reports* **4** (2010).
 22. X. Wan, J. Dong, M. Qian, and W. Zhang, "Nonlinear optical properties of perovskite ymno_3 studied by real-space recursion method," *Phys. Rev. B* **61**, 10664–10669 (2000).
-

1. Introduction

It has long been a goal of optical physicists to utilize light to control the transmission of another optical signal, and thus constructing all optical logic gates [1]. One way to achieve such control is via optical bistability, in which two distinct output optical powers can be achieved for the same input power [2]. Thus, one can control the output power by transitioning between two stable states with a minimal change in the input signal. With an increasing trend of building optical interconnects for data transfer over short distances, one can envision that optical systems could be a new means of computation, rather than simply a channel for signal transportation [3, 4]. In such optical computing networks, a bistable optical device is an essential component.

Optical bistability can be achieved in several ways, including via thermo-optic effects [5], carrier injection [6], a combination of both [7], or via optoelectronic feedback [8]. Unfortunately, all these methods are inherently slow, as they implicitly or explicitly rely on carrier generation. Another way to achieve optical bistability is via nonlinear optical effects [9]. However, nonlinear optical effects in bulk materials are often very weak, requiring large optical powers ($\sim mW$) to observe the necessary bistability [10]. This increases the power consumption of such devices and thus, limits the technological practicality. While we can select different materials with greater nonlinear susceptibilities, we can also reduce the operating optical power by increasing the strength of the nonlinear light-matter interaction itself, e.g. by using high quality (Q) factor cavities with small mode volumes. However, the need for strong nonlinearity and possibility of fabricating very high Q-cavities poses an interesting trade-off. Silicon compatible materials (i.e. silicon or silicon nitride) have long formed the foundation of electronic devices and have recently emerged as a scalable technology for photonics [11, 12]. However, these materials lack a second-order nonlinear susceptibility, which, when present, is often much stronger and subsequently, more effective in reducing the required optical input power. Silicon materials and their existing fabrication infrastructure could still form the basis for optically bistable devices if one can successfully incorporate strongly nonlinear materials with silicon photonic devices. In fact, several recently discovered materials, like transition metal dichalcogenides [13] and topological insulators [14], exhibit strong second-order nonlinear susceptibilities and can be easily integrated with silicon compatible platforms. The possibility of creating such hybrid systems consisting of strongly nonlinear materials integrated with a silicon compatible optical cavity, presents an opportunity to revisit the problem of low power optical bistability, based on second-order nonlinearity. In this paper, we seek to theoretically explore the lower limits of operating optical powers at which one can achieve optical bistability. Specifically, we analyze how the required optical power scales with cavity parameters as well as examine switching speeds by modeling the dynamics of the bistable switch.

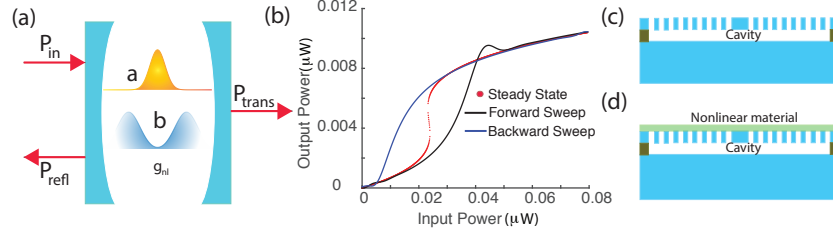


Fig. 1: (a) Schematic of a cavity with two modes with nonlinear interaction g_{nl} . The losses in the cavity primarily arise from the leak rates in the reflection (κ_{ra}) and transmission (κ_{ta}) ports. There can be additional absorptive loss, which is neglected in our analysis. (b) At steady state, the output optical power is a bistable function of the input optical power. In practice, however, one observes a hysteric behavior, depending on whether the input power is increased or decreased. The parameters for the simulation are: $g_{nl}/2\pi = 20$ GHz; $\kappa_{ta}/2\pi = \kappa_{ra}/2\pi = 3$ GHz and $\Delta_a/\kappa_a = 8$. (c) and (d) show different geometry of the nonlinear cavity: the cavity can itself be made of nonlinear material (c), or the cavity can be linear unto second-order, i.e., no $\chi^{(2)}$ nonlinearity, but with a nonlinear material (e.g. 2D material or topological insulator) transferred on top of the cavity (d).

2. Theoretical model

As explained before, in this paper, we limit our focus to second-order nonlinear optical effects. A similar model for third-order nonlinearity, where four wave mixing can give rise to optical bistability, is outlined in the appendix. The second-order nonlinear process relates two photons at the fundamental frequency to a photon at the second harmonic frequency. Since this device mediates an interaction between two different frequencies, one needs to ensure phase matching between the modes at both frequencies [15]. In a cavity structure, this equates to a non-zero spatial overlap between the cavity modes at the fundamental and the second harmonic frequencies [16, 17]. However, as we show below, in the bistable device, both input and output light are at the fundamental mode frequency, while the second harmonic mode just mediates the nonlinear interaction. We emphasize that, this is fundamentally different from a third-order nonlinear cavity, where no such phase matching is required to observe optical bistability.

The dynamics of a nonlinear cavity with multiple resonances (at the fundamental frequency ω_a and second harmonic frequency ω_b) can be described by the Hamiltonian [18]:

$$\hat{H}_s = \hbar\omega_a a^\dagger a + \hbar\omega_b b^\dagger b + \hbar g_{nl} [b(a^\dagger)^2 + b^\dagger a^2]. \quad (1)$$

The coupling constant, g_{nl} , can be expressed in terms of the classical electric fields as [18]:

$$g_{nl} = D\epsilon_0 \left(\frac{\omega_a}{2\epsilon_0} \right) \sqrt{\frac{\hbar\omega_b}{2\epsilon_0}} \int d\mathbf{r} \frac{\chi^{(2)}(\mathbf{r})}{[\epsilon(\mathbf{r})]^{3/2}} \alpha_a^2(\mathbf{r}) \alpha_b(\mathbf{r}). \quad (2)$$

Here, a and b are the annihilation operators for the fundamental and second harmonic modes, respectively; D is a degeneracy factor, describing the number of terms in the $\chi^{(2)}$ tensor that contribute to the nonlinearity; α_a and α_b are the normalized field profiles of the cavity modes such that the field-squared and integrated over the whole volume is unity, i.e., $\int |\alpha_{a,b}|^2 d\mathbf{r} = 1$. The volume integration in the expression of g_{nl} , however, should be performed only over the space where there is a nonlinear material present. Such distinction is particularly important in a hybrid system, where a transition metal dichalcogenide or topological insulator are placed on top of an otherwise linear silicon or silicon nitride cavity, e.g., see Fig. 1(d). Assuming $\omega_b = 2\omega_a$, $D = 2$ and a perfect overlap between the cavity modes ($\alpha_a(r) = \alpha_b(r) = \alpha(r)$), we find that the nonlinear interaction term reduces to

$$\hbar g_{nl} = \epsilon_0 \left(\frac{\hbar\omega_a}{\epsilon_0\epsilon_r} \right)^{3/2} \frac{\chi^{(2)}}{\sqrt{V_m}} \quad (3)$$

where, $1/\sqrt{V_m} = \int_{NL} \alpha^3(r) dr$. Note that, the phase matching condition is implicit in the assumption of perfect overlap between the cavity modes. The input light can be modeled as driving the fundamental mode, a , by adding the term $\sqrt{2\kappa_{ra}}E(e^{-i\omega_l t} a + e^{i\omega_l t} a^\dagger)$ to the Hamiltonian. E denotes the amplitude of the electric field of the driving laser, ω_l is the laser frequency, and κ_{ra} is the incoupling rate of the cavity mode a associated with the reflectance from the cavity. By transforming to a rotating frame (as the optical frequencies are much larger than the cavity loss rate or the nonlinear interaction strength) [19], we can write

$$H_{rot} = \hbar\Delta_a a^\dagger a + \hbar\Delta_b b^\dagger b + \hbar g_{nl}[b(a^\dagger)^2 + b^\dagger a^2] + \sqrt{2\kappa_{ra}}E(a^\dagger + a). \quad (4)$$

In this representation, $\Delta_{a,b}$ describes the detuning of each cavity mode from the laser frequency. With a Hamiltonian, however, we can study only the lossless evolution of the system, whereas, a realistic system is lossy. All the cavity losses (from mirror losses and material absorption) can be incorporated by including the Lindblad terms in the Master equation describing the evolution of the density matrix, ρ of the double cavity system, as [20]:

$$\frac{d\rho}{dt} = -i[H_{rot}, \rho] + \sum_{i=a,b} \kappa_i [2A_i \rho A_i^\dagger - A_i^\dagger A_i \rho - \rho A_i^\dagger A_i]. \quad (5)$$

Here A_i represents the annihilation operators for either mode, a or b . Note that, for each of these cavity modes, we have assumed there are three loss channels: reflection, transmission and absorption, with field decay rates denoted as $\kappa_{ra,rb}$, $\kappa_{ta,tb}$ and $\kappa_{la,lb}$, respectively (Fig. 1(a)). The total photon-loss rate for each cavity mode is then given by $\kappa_{a,b} = \kappa_{ta,tb} + \kappa_{ra,rb} + \kappa_{la,lb}$. Using the relation $\frac{d\langle A_i \rangle}{dt} = Tr[A_i \frac{d\rho}{dt}]$, we derive the mean-field equations for the cavity fields:

$$\frac{d\langle a \rangle}{dt} = i\Delta_a \langle a \rangle - (\kappa_{ra} + \kappa_{ta} + \kappa_{la}) \langle a \rangle - 2ig_{nl} \langle ba^\dagger \rangle + i\sqrt{2\kappa_{ra}}E, \quad (6)$$

$$\frac{d\langle b \rangle}{dt} = i\Delta_b \langle b \rangle - (\kappa_{rb} + \kappa_{tb} + \kappa_{lb}) \langle b \rangle - ig_{nl} \langle a^2 \rangle. \quad (7)$$

Where $\langle A_i \rangle$ is a complex number denoting the expectation value of the operator A_i . One can numerically solve these mean-field equations to analyze the behavior of the nonlinear cavity. We however want to first understand the condition for optical bistability in the nonlinear system at the steady state. If $\omega_b = 2\omega_a$, then the rotating frame implies that $\Delta_b = 2\Delta_a$ [18]. Furthermore, for the sake of simplicity we also assume that the quality factors of our cavity modes are identical at frequencies ω_a and ω_b leading to $\kappa_b = 2\kappa_a$. Therefore, in the steady state, by eliminating the mode b (from Eqn. 6 we can derive:

$$\eta^2 P_{trans}^3 + 2\eta(\kappa_a^2 - \Delta_a^2) P_{trans}^2 + (\Delta_a^2 + \kappa_a^2)^2 P_{trans} = 4\kappa_{ta}\kappa_{ra}(\Delta_a^2 + \kappa_a^2) P_{in}, \quad (8)$$

where $\eta = g_{nl}^2/2\kappa_{ta}$, $P_{trans} = 2\kappa_{ta} \langle a^\dagger a \rangle$ is the transmitted power from the fundamental cavity mode, $P_{in} = E^2$ is the input optical power and the intra-cavity photon number is given by $N_c = \langle a^\dagger a \rangle$. The assumption of $\Delta_b - i\kappa_b = 2(\Delta_a - i\kappa_a)$ is however difficult to achieve in the current technology and the effect of mismatch is analyzed in the appendix. However, the overall behavior of the bistable system does not change significantly when this condition is not satisfied. Note that P_{trans} , as mentioned so far, does not have units of power, but rather photons per second. To obtain the actual power, we need to multiply P_{trans} and P_{in} by the corresponding photon energy $\hbar\omega_a$. Eq. (8), which describes the steady state behavior of the fundamental cavity mode, is a cubic equation (when $\eta \neq 0$) and exhibits bistable behavior as long as $|\Delta_a| \geq (2 + \sqrt{3})\kappa_a$ (see Appendix), irrespective of the magnitude of η determined by the nonlinear interaction strength. However, η determines the input power at which the bistability appears. Simple inspection of Eq. (8) shows that by increasing η (e.g. by increasing the nonlinear coupling strength or by

decreasing the transmission of the fundamental mode), one can decrease the required optical power by several orders of magnitude. We emphasize that η can also be interpreted as the strength of the positive feedback to observe the bistability, as explained in Ref. [8].

In a realistic dielectric cavity, the cavity loss primarily arises from loss in the transmission and reflection ports and one can neglect the absorptive loss. Moreover, the transmission and reflection ports are generally equivalent leading to $\kappa_{ta} = \kappa_{ra} = \kappa_a/2$. Under these assumptions we can simplify Eq. (8) to

$$\eta^2 P_{trans}^3 + 2\eta(\kappa_a^2 - \Delta_a^2)P_{trans}^2 + (\Delta_a^2 + \kappa_a^2)^2 P_{trans} = \kappa_a^2(\Delta_a^2 + \kappa_a^2)P_{in}. \quad (9)$$

This assumption is used for all the numerical simulations present in the paper.

As previously discussed, optically bistable devices allow for large swings in the output power with slight changes to the input power. The steady state behavior of the input and output power as predicted by Eq. (8) shows two different values of P_{trans} for the same P_{in} over a range of input powers. In practice, however, such steady-state behavior is never observed. The bistable behavior manifests itself by a sudden jump of P_{trans} between the two steady-state values, with slight changes in P_{in} . Depending on whether P_{in} is increasing or decreasing, we observe different behavior in the output power, characteristic of hysteretic behavior and a bistable system (see Fig. 1(b)). The critical points of the bistable system, where we observe sudden changes in output power from slight changes in the input power can be found by solving $dP_{in}/dP_{trans} = 0$. These critical points are important to qualitatively understand the scaling of the optical power for the bistable system. To observe optical bistability, one typically requires a large laser detuning, relative to the loss rate. Thus, when $\Delta_a \gg \kappa_a$, we yield critical points at $P_{trans} = \Delta_a^2/\eta$ and $\Delta_a^2/3\eta$ corresponding to the input powers $P_{in} = 0$ and $4\Delta_a^4/27\eta\kappa_a^2$. This indicates that the signal swing is $\sim \kappa_a^2/\Delta_a^2$. From the expression of the critical input power $P_{in} = 4\Delta_a^4/27\eta\kappa_a^2$, we can clearly see that with an increasing η , the required power to observe bistability decreases, as pointed out earlier in the paper. The critical input power also scales with the detuning and cavity loss as $\sim \Delta_a^4/\kappa_a^2$. From our previous analysis, we also found out that to observe the bistability, the condition $|\Delta_a| > (2 + \sqrt{3})\kappa_a$ needs to be satisfied. Hence, the input optical power where one can observe optical bistability scales as $\sim \kappa_a^3/g_{nl}^2 \sim V_m/Q^3$. We emphasize that, such scaling is more favorable for lowering the optical power by using a high-Q cavity, compared to other cavity-based bistable devices employing photo-refractive or thermo-optic effects, where the input power typically scales as $\sim V_m/Q$ [6].

3. Performance of the switch

Using this model, we now analyze the performance of an optical switch based on the bistable device. The input signal consists of a fixed bias power P_{bias} and a modulated optical signal. For the best operation, P_{bias} should be in the grey region in Fig. 2(a). The modulated input signal is changed sinusoidally with a frequency Ω and amplitude, P_{amp} . This will modulate the output power with the same frequency, but a different amplitude. We define the ratio of the output and input power amplitude as the gain, G , of the switch. As discussed earlier, the output signal swing is proportional to κ_a^2/Δ_a^2 , and for all subsequent analysis, we will let $\Delta_a/\kappa_a = 8$. We analyze G as a function of P_{bias} and P_{amp} for a modulation frequency of $\Omega/2\pi = 500$ MHz and find that the gain increases with decreasing P_{amp} (Fig. 2(b)). A bistable system can only swing between its two steady states, and by increasing P_{amp} , the output swing cannot be increased indefinitely. Hence a reduced P_{amp} increases the gain. At a very low value of P_{amp} , however, the system cannot switch, and the output becomes distorted (not shown here). Although, a large gain is desired for a good optical switch, we also want to have a large range of bias-points, i.e. absence of critical biasing [3]. This means we should have a range of P_{bias} , where a high gain can be achieved. Figure 2(b) clearly shows that this range decreases with decreasing P_{amp} . Hence to

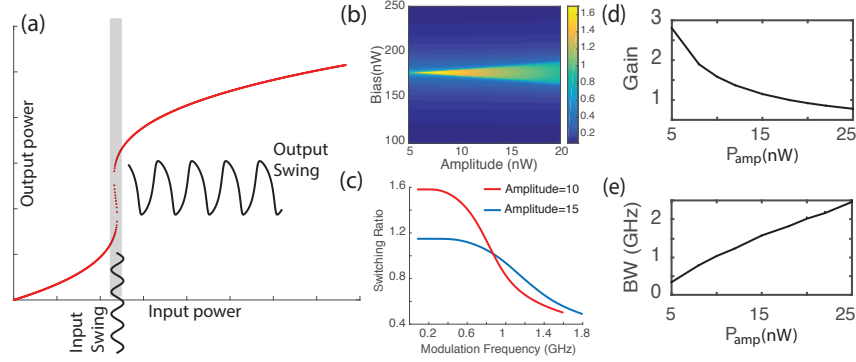


Fig. 2: (a) The steady state bistability plot is used to identify the bias-points, around which one can modulate the input power to observe the change in the output power. (b) The ratio between the output power amplitude and input power amplitude as a function of P_{bias} and P_{amp} . (c) The frequency response for two different P_{amp} , showing the bandwidth changes depending on the amplitude. (d) Gain, defined as the switching ratio at a low frequency, (e) Bandwidth, defined at the 3 dB point, is plotted as a function of the P_{amp} . The parameters for the simulation are: $g_{nl}/2\pi = 20$ GHz; $\kappa_a/2\pi = \kappa_{ra}/2\pi = 3$ GHz and $\Delta_a/\kappa_a = 8$.

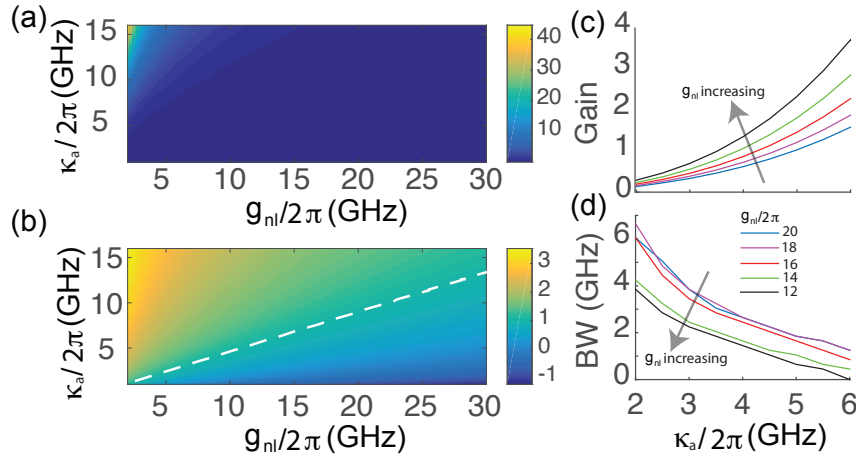


Fig. 3: (a) The bias point P_{bias} as a function of the total linewidth $2\kappa_a$ and nonlinear interaction strength g_{nl} . (b) $\log_{10}(N)$, N being the intra-cavity photon number plotted as a function of κ_a and g_{nl} . (c) Gain as a function of κ_a for different g_{nl} . (d) Bandwidth as a function of κ for different g_{nl} .

avoid critical biasing, one needs a P_{amp} that is significantly larger than the absolute minimum P_{amp} needed to switch between the two states.

By changing the modulation frequency, Ω , we find that the switch behaves as a low-pass filter (Fig. 2(c)). However, the frequency response depends on the input amplitude P_{amp} . To understand such dependency, we analyze the frequency response of the switch as a function of the input amplitude P_{amp} keeping all other system parameters fixed (Figs. 2(d), and 2(e)). We find that with increasing P_{amp} , the gain decreases while the bandwidth increases. The change in bandwidth can be explained qualitatively via the constancy of the gain-bandwidth product. Next, we analyze the dependence of the input optical power on the cavity loss rate κ_a and nonlinear interaction strength g_{nl} . For different system parameters, we calculate the input optical power P_{bias} where we observe the optical bistability. Figures 3(a) and 3(b) show the average P_{bias} and intra-cavity photon number $N = \langle a^\dagger a \rangle$, respectively, as a function of κ_a and g_{nl} . As previously

derived, the scaling of input optical power should follow $V_m/Q^3 \sim \kappa_a^3/g_{nl}^2$. However, the intracavity photon number N scales κ_a^2/g_{nl}^2 , as the photon number depends on the cavity loss rate κ_a . From these figures, we identify the parameter range (the region under the white line in Fig. 3(b)) where the photon number, N , is less than 10. With a nonlinear interaction strength of $g_{nl}/2\pi = 20$ GHz, and loss rate $\kappa_a/2\pi = 10$ GHz, one can reach the $N \sim 10$ photons regime. For a target wavelength of $\sim 1.5\mu\text{m}$, this entails a quality factor of $\sim 20,000$, which is readily achievable in state-of-the-art cavities. To achieve $g_{nl}/2\pi = 20$ GHz using a dielectric cavity with mode-volume $V_m \sim (\lambda/n)^3$, n being the refractive index of the cavity material, at a typical wavelength of $\lambda \sim 1.5\mu\text{m}$, the nonlinear second-order coefficient $\chi^{(2)}$ would need to be ~ 5 nm/V. This is more than one order of magnitude larger than available bulk materials. To reach the necessary nonlinearity one either needs to use a material with larger optical nonlinearity or use a cavity with small mode volume. Although metallic structures can provide a small mode volume, the excess loss due to the metal is detrimental for the ultimate performance. Hence, a better avenue will be to use new materials, like 2D materials [21], perovskites [22], or topological insulators [14] instead. Another approach could be to compensate for the reduced nonlinear interaction strength by using a high-quality factor cavity. For example, one can reach the ten-photon regime with $g_{nl}/2\pi = 1$ GHz and a cavity quality factor of ~ 200000 . Such a high quality factor is difficult to achieve in III-V materials, but can be reached in silicon cavities. This emphasizes the necessity of building the second-order nonlinear hybrid platform, as previously discussed.

Using these bias-points, we calculate the frequency response of the bistable system. Specifically, we analyze the gain at low modulation frequency as well as the bandwidth of the switch. Figure 3(c) shows the gain as a function of the linewidth $2\kappa_a$ for different g_{nl} values. A clear increase in the gain is observed with κ_a as can be explained from the simple model of gain $\sim \kappa_a^2$. From the constancy of the gain-bandwidth product, we expect the bandwidth to decrease with increasing κ_a (Fig. 3(d)). Note that such behavior is unusual for cavity based devices, where the speed is largely limited by the cavity lifetime. In those devices the speed generally increases with κ_a . Such observation is critical, as high-Q cavities are generally considered bad for high speed operation even though they are beneficial from the stand-point of power. However, for optically bistable devices, we find that increased quality factors improve the power consumption while maintaining high speed operation. The use of high-Q cavities is, however, not without drawbacks as it still poses problems for thermal stability, as well as limiting gain in the switching operation.

4. Conclusion

We have analyzed the performance of an optically bistable system based on second-order nonlinearity in terms of the power and the speed of operation via a simple dynamic classical model. We found that with high quality-factor and low mode volume V_m , one can push the energy required to observe bistability to the few photon level. The energy scales as V_m/Q^3 . Temporal analysis of the bistable switch also reveals that the speed of operation decreases with an increase in cavity linewidth, in contrast to other cavity-based devices. Such low power nonlinear operation will be useful to implement optical computing systems.

Appendix

4.1. Detailed derivation of the bistable system with $\chi^{(2)}$ nonlinearity:

Starting from the dynamic equations in the main text

$$\frac{d\langle a \rangle}{dt} = i\Delta_a \langle a \rangle - (\kappa_{ra} + \kappa_{ia} + \kappa_{la}) \langle a \rangle - 2ig_{nl} \langle b \rangle \langle a \rangle^\dagger + i\sqrt{2\kappa_{ra}} E,$$

$$\frac{d\langle b \rangle}{dt} = i\Delta_b \langle b \rangle - (\kappa_{rb} + \kappa_{lb} + \kappa_{lb}) \langle b \rangle - ig_{nl} \langle a \rangle^2.$$

we find that at the steady-state,

$$\langle b \rangle = \frac{ig_{nl} \langle a \rangle^2}{i\Delta_b - (\kappa_{rb} + \kappa_{lb} + \kappa_{lb})}$$

Using this we can write the equation for operator a (at steady state) as:

$$i\Delta_a \langle a \rangle - (\kappa_{ra} + \kappa_{la} + \kappa_{la}) \langle a \rangle + \frac{2g_{nl}^2}{i\Delta_b - (\kappa_{rb} + \kappa_{lb} + \kappa_{lb})} \langle a \rangle^\dagger \langle a \rangle^2 + i\sqrt{2\kappa_{ra}} E = 0$$

This can be rewritten as

$$i\Delta_a \langle a \rangle - \kappa_a \langle a \rangle + \frac{2g_{nl}^2}{i\Delta_b - \kappa_b} \frac{P_{trans}}{2\kappa_{la}} \langle a \rangle + i\sqrt{2\kappa_{ra}} E = 0$$

Assuming $2(i\Delta_a - \kappa_a) = i\Delta_b - \kappa_b$, we can write

$$\eta^2 P_{trans}^3 + 2\eta(\kappa_a^2 - \Delta_a^2) P_{trans}^2 + (\Delta_a^2 + \kappa_a^2)^2 P_{trans} = 4\kappa_{la} \kappa_{ra} (\Delta_a^2 + \kappa_a^2) P_{in},$$

The critical points are given by

$$\frac{dP_{in}}{dP_{trans}} = 3\eta^2 P_{trans}^2 + 4\eta(\kappa_a^2 - \Delta_a^2) P_{trans} + (\kappa_a^2 + \Delta_a^2)^2 = 0$$

The system is bistable as long as $16\eta^2(\kappa_a^2 - \Delta_a^2)^2 - 12\eta^2(\kappa_a^2 + \Delta_a^2)^2 = 4\eta^2(\kappa_a^4 + \Delta_a^4 - 14\kappa_a^2\Delta_a^2) > 0$. This condition can be simplified to the criteria: $|\Delta_a| < (2 + \sqrt{3})\kappa_a$. The critical points are given by

$$P_{trans}^{cr} = \frac{2(\Delta_a^2 - \kappa_a^2) \pm \sqrt{\kappa_a^4 + \Delta_a^4 - 14\kappa_a^2\Delta_a^2}}{3\eta}$$

These critical points are involved and provide little intuition. To qualitatively understand the system behavior, we assume lossless cavity with $\kappa_{la} = \kappa_{ra} = \kappa_a/2$ and $\Delta_a \gg \kappa_a$ and simplify the equation as:

$$\eta^2 P_{trans}^3 - 2\eta\Delta_a^2 P_{trans}^2 + \Delta_a^4 P_{trans} = \kappa_a^2 \Delta_a^2 P_{in}$$

Here the critical points are the roots of

$$3\eta^2 P_{trans}^2 - 4\eta\Delta_a^2 P_{trans} + \Delta_a^4 = 0$$

From this we calculate the critical points as previously reported.

4.2. Optical bistability in a cavity with third order nonlinear material:

We assume a third order nonlinear cavity driven by an external laser. The Hamiltonian of the driven system is given by

$$\mathcal{H} = \Delta a^\dagger a + \chi a^\dagger a a + \sqrt{2\kappa_r} E (a + a^\dagger)$$

From the master equation (with losses added via the Lindblad formalism), the mean-field equations for the cavity annihilation operator a as:

$$\frac{da}{dt} = Tr \left[a \frac{d\rho}{dt} \right] = i\Delta a - (\kappa_r + \kappa_l + \kappa_l) a + 2i\chi a^\dagger a a + i\sqrt{2\kappa_r} E$$

The different output powers are given by $P_{trans} = 2\kappa_l a^\dagger a$; $P_{loss} = 2\kappa_l a^\dagger a$ and $P_{refl} = 2\kappa_r a^\dagger a$. At steady state we can write

$$i\Delta a - (\kappa_r + \kappa_l + \kappa_l)a + 2i\chi a^\dagger a a + i\sqrt{2\kappa_r}E = 0$$

This can be simplified to

$$a = -\frac{i\sqrt{2\kappa_r}E}{i\left(\Delta + \frac{\chi P_{trans}}{\kappa_l}\right) - (\kappa_r + \kappa_l + \kappa_l)}$$

The transmitted power at steady state becomes:

$$P_{trans} = \frac{4\kappa_l \kappa_r |E|^2}{\left(\Delta + \frac{\chi P_{trans}}{\kappa_l}\right)^2 + (\kappa_r + \kappa_l + \kappa_l)^2}$$

Denoting $\eta = \chi/\kappa_l$, the equation can be written as

$$\eta^2 P_{trans}^3 + 2\Delta\eta P_{trans}^2 + P_{trans}(\Delta^2 + (\kappa_r + \kappa_l + \kappa_l)^2) - 4\kappa_r \kappa_l P_{in} = 0$$

The critical points can be found out by solving

$$\frac{dP_{in}}{dP_{trans}} = 3\eta^2 P_{trans}^2 + 4\Delta\eta P_{trans} + \Delta^2 + (\kappa_r + \kappa_l + \kappa_l)^2 = 0$$

and critical points are

$$P_{trans}^{cr} = \frac{-2\Delta \pm \sqrt{\Delta^2 - 3\kappa^2}}{3\eta}$$

$$P_{in}^{cr} = \frac{-2\Delta(\Delta^2 + 9\kappa^2) \mp 2(\Delta^2 - 3\kappa^2)^3}{108\eta \kappa_l \kappa_r}$$

4.3. Effect of different quality factors in $\chi^{(2)}$ nonlinear cavities:

In the main text of the paper we assumed that $\Delta_b - i\kappa_b = 2(\Delta_a - i\kappa_a)$, which is based on the assumptions that the mode near second harmonic frequency is exactly twice the fundamental frequency and the Q-factor of both cavities are exactly same. However, such assumptions do not always hold true. Without such an assumption the governing equation looks like:

$$4\eta^2 P_{trans}^3 + 4\eta(\kappa_a \kappa_b - \Delta_a \Delta_b) P_{trans}^2 + (\kappa_a^2 + \Delta_a^2)(\kappa_b^2 + \Delta_b^2) P_{trans} = 4\kappa_a \kappa_b (\Delta_b^2 + \kappa_b^2) P_{in} \quad (10)$$

Using similar procedures as explained before, the critical points are given by

$$P_{trans}^{cr} = \frac{\kappa_a \kappa_b}{6\eta} \left[\left(\frac{\Delta_a \Delta_b}{\kappa_a \kappa_b} - 1 \right) \pm \sqrt{\left(1 - \frac{\Delta_a \Delta_b}{\kappa_a \kappa_b} \right)^2 - 3 \left(\frac{\Delta_a}{\kappa_a} + \frac{\Delta_b}{\kappa_b} \right)^2} \right] \quad (11)$$

We note that, to observe the bistability, one needs to satisfy the condition,

$$\left| \frac{\Delta_a \Delta_b}{\kappa_a \kappa_b} - 1 \right| \geq \sqrt{3} \left| \frac{\Delta_a}{\kappa_a} + \frac{\Delta_b}{\kappa_b} \right| \quad (12)$$

Note that, even if a condition $\Delta_b - i\kappa_b = 2(\Delta_a - i\kappa_a)$ is difficult to satisfy one can easily achieve $\frac{\Delta_a}{\kappa_a} \approx \frac{\Delta_b}{\kappa_b}$. This means, the bistability condition becomes

$$\frac{\Delta_a}{\kappa_a} \approx \frac{\Delta_b}{\kappa_b} \geq 2 + \sqrt{3} \quad (13)$$

Hence, we find that even if the quality factor of the second harmonic mode can be worse than the fundamental mode, as long as similar ratio between the detuning and the linewidth for the two modes. Under the assumptions $\Delta_a \gg \kappa_a$, $\Delta_b \gg \kappa_b$ and $\kappa_{ra} = \kappa_{ta} = \kappa_a/2$, the critical points are $P_{trans} = \Delta_a \Delta_b / 6\eta$ and $\Delta_a \Delta_b / 2\eta$ corresponding to the input powers of $P_{in} = 0$ and $2\Delta_a^3 \Delta_b / 27\eta \kappa_a^2$. Hence the input power scales as $P_{in} \sim \Delta_a^3 \Delta_b / \eta \kappa_a^2$. This shows that, the input power increases with a lower quality factor of the second harmonic mode, as it depends on Δ_b .

Acknowledgments

This work is supported by the National Science Foundation under grant NSF-EFRI-1433496 and the Air Force Office of Scientific Research under grant FA9550-15-1-0150. CD is supported by the startup fund provided by University of Washington, Seattle.